Airflow Measurement Techniques for the Improvement of Forced-air Cooling, Refrigeration and Drying Operations

Justin O'Sullivan[1], Maria Ferrua[2], Richard Love[1], Pieter Verboven[3], Bart Nicolaï[3], and Andrew East[1]

[1]Centre for Postharvest and Refrigeration Research, Massey University, Private Bag 11-222, Palmerston North 4442, New Zealand, Ph +64 6 350 4336; Fax +64 6 350 5657

[2]Riddet Institute, Massey University, Private Bag 11-222, Palmerston North 4442, New Zealand

[3]BIOSYST-MeBioS, University of Leuven, Willem de Croylaan 42, Heverlee, Belgium

Abstract

Flowrate and distribution of air is a critical design factor in the cooling, refrigeration and drying of horticultural food products. These operations rely on a constant supply of air distributed throughout bulk arrangements of the produce. Local distribution of the air is critical to optimizing the design and efficiency of these processes. Identification of the key parameters affecting the airflow distribution has been done either experimentally (using intrusive point-wise or bulk measurement techniques) or numerically. The detailed information provided by the use of computational fluid dynamic models has facilitated unique opportunities to investigate alternative system designs, without the need for expensive and time consuming experiments. This study provides a review of the techniques available to measure airflow (thermal and rotatory vane anemometry, pressure differential devices, tracer gases, LDA and PIV). Their advantages and disadvantages (accuracy, resolution, application range, cost, and ease of use) as well as their application in the validation of numerical models are reviewed. The novel and scientifically based design guidelines developed by a better understanding of the airflow behaviour within the system for each of the operations under study are also presented.

Keywords: numerical model validation; experimental; laser doppler anemometry; particle image velocimetry; thermal anemometry; flow visualisation.

1. Introduction

Common cooling and drying operations of food are typically based on the heat exchange between a food product and a constant supply of airflow through the system (Ghisalberti and Kondjoyan, 1999). For the cooling, refrigeration and drying of food the flowrate, distribution and temperature of the airflow throughout the entire packaging structure ultimately determines the rate, uniformity and efficiency of these processes. As uniform temperatures are desired in all three operations any operating and/or design feature capable of affecting the local distribution of the airflow behaviour within the system will have a profound effect on the performance of these processes.

In forced-air cooling, the size and location of the openings of the ventilated packages have been found to have a particular effect on the rate and uniformity of the process (Defraeye et al., 2013; Defraeye et al., 2014; Delele et al., 2008; Ferrua and Singh, 2009a; van der Sman, 2002; Vigneault et al., 2006). Ventilated packaging should be designed to provide uniform airflow distribution. However, uniform cooling does not always go hand in hand with higher cooling rates, and package design is a determining factor (Defraeye et al., 2014). The vents or openings determine how much air can come in contact with the product, how it is distributed inside the package, and what the air velocity magnitude is. Hence, cooling heterogeneity within packages is often a result of uneven airflow distribution (Dehghannya et al., 2008;

2011; 2012). A comprehensive review by Pathare et al. (2012) gives the recommended vent areas for a wide range of ventilated packages for horticultural produce.

In refrigerated rooms pallet stacking patterns can result in an uneven airflow distribution. When pallets are stacked high and closely packed together those centrally located and at the rear of the room (away from the evaporator fans) will receive smaller volumetric flows of refrigerated air compared to the pallets at the front of the room (adjacent to the evaporator fans). These local differences in flowrate throughout the room cause differences in the air temperature, with warm spots developing depending on pallet location (Verboven et al., 2003). Similarly, for refrigerated transport vehicles, pallet compactness can lead to high airflow resistances and uneven airflow distribution, with the formation of stagnant zones with higher air temperatures in the rear of the vehicle (Smale et al., 2006).

Typically, in forced-convection drying, warm, dry air exits an inlet and is distributed under a bed of horticultural produce. This air tends to follow a streamline flow and if not redirected will be distributed along the centre and towards the back of system, with regions not in the main pathway receiving smaller volumetric airflows, resulting in a non-uniform final moisture content (Nagle et al., 2010). When using impinging hot air jets for drying, the location and direction of the jet can affect the rates of heat and mass transfer spatially along the product width, as a higher percentage of the airflow is directed to one section of the product (Marcroft et al., 1999).

To improve the performance of these food operations a detailed understanding of how different design parameters and operating conditions affect the airflow behaviour within the systems is essential. This information has been traditionally obtained by measuring the local distribution of the airflow within the system using a wide range of experimental techniques. In addition, experimental information collected on the behaviour of the airflow has been also recently used for the validation of numerical models of the process (Smale et al., 2006). Beginning in the 1990s engineering simulation tools, such as Computational Fluid Dynamics (CFD), have become increasingly used in the analysis of cooling and drying processes within the food industry. Relevant examples are given in Wang et al. (2003). Advanced CFD tools can predict complex airflow patterns in food operation systems in a level of detail difficult to achieve experimentally, facilitating a better and more fundamental understanding of the effect of the design and operating conditions on the efficiency of the process.

This study reviews not only the airflow measurement techniques currently employed to characterise airflow behaviour in forced-air cooling, refrigerated and drying applications but also their application in developing a better understanding and design of these processes.

2. Airflow measurement techniques

2.1 Direct airflow measurement

Direct flow measurement techniques are generally devices placed in the flow field which measure point-values in a system. They are widely used due to their robustness, ease of use and competitive price compared to non-invasive image analysis. These techniques include thermal anemometry, vane anemometry and differential pressure flowmeters.

2.1.1 Thermal anemometers

Thermal anemometers consist of a small, electronically heated sensor, initially kept at a constant temperature above that of the fluid flow temperature. Once the sensor is placed in the flow field it experiences a certain amount of cooling. As the electrical resistance of the sensor is dependent upon its temperature, a relationship can be obtained between the flow speed and the voltage output from the sensor.

Thermal anemometers can be operated to maintain a constant temperature or constant current through the sensor. In the case of constant temperature anemometers, the sensor's resistance is constant and the required voltage (or current) to maintain the temperature is measured. Conversely, for constant current anemometers the applied current is held constant and the sensor's voltage drop (or electrical resistance) is measured (Fingerson and Freymuth, 1996). The air velocity can then be inferred from the power required to maintain the temperature or current of the sensor. The sensor placed in the fluid flow is a wire for hot-wire anemometers and a film in the case of hot-film anemometers.

Thermal anemometers can be made at a relatively low cost and when thin wires are used a high sampling frequency can be used (up to 10^5 Hz). Limitations of thermal anemometers include the requirement for regular calibration, which often involves the device been sent back to the manufacturer once a year. The recorded velocities may be affected by impurities in the fluid that adhere to the wire, interfering with the heat transfer. Thin hot wire systems while very sensitive and accurate are very fragile and need to be combined with a portable

support, positioning system, a probe calibrator, A/D converter, thermal anemometry software and a computer. Such systems can become quite expensive. For use in more industrial relevant environments, more robust (thicker hot wires) and compact solutions can be used. However, these hot wire/film anemometers are unsuitable when attempting to measure very high or low air velocities. At low air velocities (i.e. below 0.1 $m.s^{-1}$) natural convection can become prevalent and as a result heat transfer is no longer solely dominated by forced convection (Page et al., 2009).
Alternatively, at high air velocities (i.e. above 100 $m.s^{-1}$) the heat from the sensor tends to dissipate extremely quickly, reducing its sensitivity to changes in the velocity field (Jing et al., 2011).

The ability of hot-wire anemometers to capture turbulent high-frequency velocity fluctuations is limited by the sensor size. Depending on the level of turbulence the fluctuating components of the air velocity can have a broad frequency spectrum, from as low as 10^{-2} Hz to in excess of 10^{5} Hz (Webster, 2000). Robust hot wire systems (diameter between 0.5 – 1.0 mm) are unable to capture these high frequency velocity variations, however, the fluctuations do increase the heat transfer between the sensor and the air, causing the average velocity to be overestimated. To compensate for this a sensor with an extremely small diameter (~ 5 μm) and electronics that can account for the fluctuating frequencies and allow for a flat frequency response between 0 – 10^{4} Hz must be employed (Webster, 2000).

When the turbulent velocity fluctuation is more than 30 % of the average velocity the probe must be moved through the flow field at a speed high enough to compensate for sudden drops in the air velocities as a result of turbulence, a technique known as “flying hot-wire system”

(Jorgensen, 2002). This requires sufficient open space for the hot-wire anemometer, which is usually not found in food processing operations.

For accurate measurements the airflow direction must be known before the experiment is started and the sensor wire mounted perpendicular to the flow, unless otherwise stated by the manufacture (Jorgenson, 2002). In the case of 2D and 3D flows, multisensory hot-wire probes are used to measure the different components of the velocity field. Spherical hot wire probes that can measure the air speeds, while being insensitive to the airflow direction also exist (Lomas, 1986).

Despite the small diameter of the sensor the probe itself often has a length in excess of 0.5 m. This can create problems when investigating the airflow conditions within confined spaces such as in between horticultural packages stacked in a pallet, as the introduction of a thermal anemometer may change the airflow conditions within them (Alvarez and Flick, 1999a).

Examples of hot-wire anemometry for measuring airflow measurements in food operations include: Alvarez and Flick, 1999a; Amanlou and Zomordian, 2011; Delele et al., 2008; 2009a; 2009b; Janjai et al., 2006; Kashaninejad et al., 2010; Ngcobo et al., 2013; Santonico et al., 2010; Verboven et al., 2005.

2.1.2 Vane anemometry

Vane anemometers measure the average velocity of the airflow of a particular region within a system. A vane anemometer operates on the principle that when fluid flow hits the vanes it causes them to rotate. The higher the flow speed the faster the rotation. This rotational speed is sensed by an optical or magnetic sensor and the signal is converted to a velocity measurement.

The simplicity of vane anemometers has resulted in the manufacturing of hand held devices, which are advantageous if a portable measurement device is required. The accuracy of the anemometer is heavily dependent on the vane angle with respect to the airflow direction, which must be precisely known before any velocity measurements can be taken (Mirade, 1998). Additionally, there is a minimal threshold velocity required to cause initial rotation of the vanes.

The relatively bulky size of vane anemometers renders them as an unsuitable selection for use within small void spaces (e.g. horticultural produce packaging), but is a viable method for measuring the airflow in larger spaces such as before or after it encounters horticultural produce.

Examples of vane anemometry for measuring airflow measurements in food measurements include: Hossain and Bala, 2007; Lawrence and Maier, 2011; Kadam et al., 2008; Motevali, 2013; Nagle et al., 2010.

2.1.3 Differential pressure flowmeters

Differential pressure flow meters determine the flow velocity by either measuring the pressure losses over obstructions of known dimensions, such as orifice plates and Venturi meters, or by calculating the different pressure components (Coulson et al., 1999).

The devices used to record pressure differences can be classified into U-tube manometers and pressure transducers. U-tube manometers are simple to construct. However, they are not suitable when it comes to measuring very low flow rates and cannot be used in unsteady-state systems. In the case of very low rates the accuracy of the small pressure differences to be evaluated could be compromised. If the system is in transient operation the pressure difference, measured by the height difference of the fluid within each port of the U-tube, will be constantly fluctuating, making it difficult to record a single value.

Unlike U-tube manometers, pressure transducers operate by converting a pressure difference to an electrical signal that can be recorded on a data acquisition system. This represents an advantage over the U-tube manometer as it facilitates the automatic recording of pressure, including instantaneous fluctuations. They are also smaller than U-tube manometers and can operate with low airflow volumes.

Pressure devices can’t provide unobtrusive measurements of the flow in packed domains and they can only measure unidirectional flows along a streamline. Their sensitivity is limited, as they require a reasonable flowrate, to cause a detectable pressure difference. Taking the Pitot tube as an example if the flowrate is 0.6 $m.s^{-1}$ and an accuracy of 1% is required in its determination, then the manometer must be sensitive to changes of approximately 0.02 mm of a water column (Rathakrishnan, 2007). Practically, if a water column height change of 1 mm is the limiting sensitivity then the corresponding minimum air velocity that can be measured is 4 $m.s^{-1}$. Hence, pressure devices cannot be used in room cooling or storage facilities, where low velocity and stagnant zones may exist. Due to their intrusive characteristics pressure measuring devices are generally used to measure the total flow rate into or out of a system and not within it.

Examples of differential pressure flowmeters for measuring airflow measurements in food operations include: Dehghannya et al., 2008; 2011; 2012; Gill et al., 2012; Khatchatourian et al., 2009; Mohanraj and Chandrasekar, 2008; Ngcobo et al., 2012; O'Sullivan et al., 2013.

2.2. Non-invasive qualitative methods

Non-invasive flow visualisation techniques have been pivotal in developing a better understanding of postharvest cooling and refrigeration processes, as they facilitate a more detailed and accurate assessment of airflow behaviour throughout the system. By introducing visible particles (e.g. smoke) in the flow these methods can not only provide a better understanding of the flow patterns generated within the system but also facilitate a quantitative assessment (as discussed in the next section).

Smoke and helium bubbles make up the most common seeding particles to visualise airflow (Maghirand and Manbeck, 1993; Ruegg et al., 1994). The motion of the particles, within an illuminated thin laser light sheet is measured by tracking their location in time by a camera situated normal to the plane. The tracer particles must be sufficiently small and light so they can closely follow the flow field behaviour but large enough, so they scatter a sufficient amount of light, to be photographed or recorded with a camera.

Tracer particles are commonly generated by using a smoke-wire technique (Lohan, 2002; Wang et al., 2000). “Smoke” is generated by vaporising oil from a small diameter wire (~0.1 mm) through a resistive heating (Cornaro et al., 1999). Commonly used wire materials include steel and tungsten. This technique is limited to situations where the Reynolds number, based on the wire diameter, is small, approximately 20 since the smoke will become too dispersed in the fluid if the Reynolds number is higher. In practice, this low Reynolds number limitation restricts airflow experiments to maximum velocities of approximately 3 $m.s^{-1}$ (Rathakrishnan, 2007).
Smoke particles can also be generated by commercially available generators which vaporise a glycerine or alcohol solution, forming a non-toxic smoke.

The helium bubble method represents a flow visualisation technique that can be used in systems with airflow speeds of up to 60 $m.s^{-1}$ and moderate levels of turbulence (Rathakrishnan, 2007). Unlike smoke particles they can still be visualised even when dispersed. Filling soap bubbles with helium allows both the size (typically 1-3 mm) and buoyancy to be controlled, making it an ideal tracing particle (Biwole et al., 2009; Klimentjew et al., 2010; Suzuki and Kasagi, 2000). However, these bubbles tend to only reflect about 5% of incident light (Mueller, 1996), resulting in increasing importance of placement of light sources. Using the maximum possible amount of light on the bubbles, while maintaining a dark background, assists in bubble visualisation (Randall, 1979).

Examples of flow visualisation to identify flow patterns in food operations include: Hellickson et al., 2003; Sarkar and Singh, 2004.

2.3. Non-invasive quantitative methods

Non-invasive quantitative techniques expand upon flow visualisation by quantifying particles displacement. Examples of this technique that have been used to investigate the airflow behaviour during forced-air cooling, refrigeration and drying operations are tracer gas methods, laser doppler anemometry (LDA) and particle image velocimetry (PIV). These techniques do not interfere with airflow and, in the case of LDA and PIV, can be extremely accurate.

2.3.1 Tracer gas methods

Tracer gas methods determine the air movement in a system by measuring the concentration of the gas at a specific point downstream from its release into the system. Available techniques include decay, constant injection and constant-concentration measurements (Sherman, 1990). The tracer decay technique infers the flow rate by measuring the temporal drop in tracer concentration. In constant injection a uniform concentration of tracer is continuously injected and the flow determined by measuring its concentration at specific points within the domain. In constant-concentration the amount of the injected tracer is controlled to ensure a constant concentration of the tracer at a particular location. The fluid flow rate is then calculated from the required flow rate of the tracer injected divided by the concentration of the tracer (mol tracer/mol air). The tracer (gas) itself must be safe and freely available (Smale, 2004). The most common tracer gas to fit these requirements is carbon dioxide (Yan et al., 2009). However, in situations where natural convection is likely to occur, such as the static cooling of horticultural produce, carbon monoxide becomes a better choice than carbon dioxide (Amos, 2005). The airflow pattern is then analysed from time profiles of gas concentration at different positions in the system.

The tracer gas method requires sensors with fast response times and a sufficiently small size to avoid interfering with the airflow pattern (as they need to be located in different spatial positions within the system). Tracer gases are not suitable for use in a system where measurements are required over an extended time period, due to the volume of tracer required. The errors in this technique are typically in the range of 5-10% (McWilliams, 2003).

Examples of the tracer method for measuring airflow measurements in food operations include: Amin et al., 2009; 2010; 2011; 2012; Amos, 2005; Tanner et al., 2000.

2.3.2 Laser Doppler Anemometry

Both LDA and PIV are based on the analysis of movement of small (neutrally buoyant) tracer particles, which are seeded in the flow. In LDA laser light of a known frequency illuminates the particles in the air flow and the scattered light is detected by a photomultiplier tube. The principle behind LDA is that when light is reflected from a moving object the frequency of the scattered light will be altered in proportion to the speed of the object under investigation. By observing the frequency shift, the speed of the object can be estimated (Durst et al., 1981). This process is graphically presented in Figure 1.

LDA measurements are linear with velocity and the device does not require external calibration (Wu et al., 2007). LDA can measure a wide range of velocities, from 10^{-4} m.s^{-1} to

10^3 m.s^{-1}. It possesses a high frequency response and is insensitive to fluid temperature, density or composition. However, only a single point can be sampled at any given time.

Examples of LDA for measuring airflow measurements in food operations include: Alvarez et al., 2003; Foster et al., 2002; Macroft et al., 1999; Macroft & Karwe, 1999; Moureh et al., 2004, 2009a, 2009b, 2009c.

2.3.3 Particle image velocimetry

In PIV the flow is successively illuminated by thin layers of laser light, within a short period of time. The location of the particles is then determined within each laser pulse by measuring the light scattered by them into a CCD (Charge Coupled Device) camera. Once the location of the particles is determined for each laser pulse the particle displacement is then determined by cross-connecting their location in two successive laser pulses. From these correlations, a velocity vector can be obtained for each small region of the imaged domain, resulting in a vector field (Adrian, R., 1991). For a comprehensive and more detailed explanation of the PIV technique, the reader is referred to Prasad (2000). The PIV technique is illustrated in Figure 2.

PIV has advantages compared to LDA in that it is a whole-flow-field measurement technique that provides instantaneous velocity vector measurements in an entire cross-section of the fluid flow, as opposed to the single point measurements associated with LDA. Planer flows, as well as 3D flows can be obtained and continued advances in the acquisition frequency of digital cameras have facilitated the assessment of turbulent structures in greater detail.

For LDA and PIV a clear line of sight (e.g. transparent window) must be provided to the fluid flow so the movement of the tracer particles can be recorded. Unlike the tracer gas method, LDA and PIV require an unobstructed view of the point being measured, reducing their applicability in actual food processing rooms filled with produce (Amos, 2005). This requirement has meant that although LDA and PIV have been used extensively in aerodynamics (Jeffrey et al., 2000; Raffel and Kost., 1998) and biomechanics (Gijsen et al., 1996; Lim et al., 2001) it is only recently that the techniques have been applied to complex flow systems found in food operations. LDA and PIV are also relatively expensive techniques.

Examples of PIV for measuring airflow measurements in food operations include: Laguerre et al., 2008; 2009; 2010; 2012; Ferrua and Singh, 2008; 2009a; 2009b; 2009c; 2011.

3. Design and efficiency of post-harvest cooling

3.1 Forced-air cooling

In forced-air cooling field heat is removed from freshly harvested produce by placing the produce inside palletised ventilated packages through which refrigerated air, at relatively high flow rates, is forced through by means of a fan (Figure 3) (Brosnan and Sun, 2001). For the tunnel cooler, the most common forced-air cooling device, the fan creates a vacuum which draws refrigerated air through two palletized rows of horticulture produce.

As refrigerated air is pulled through ventilated packages preferential airflow pathway are formed, along with areas of maximum and minimum airflow velocities (Alvarez and Flick, 1999a, 2003). This uneven distribution of the refrigerated air leads to cooling heterogeneity within the packages.

Alvarez and Flick (1999a) conducted an experimental aerodynamic study to better understand the relationship between the cooling heterogeneity during the forced-air cooling process and the behaviour of the airflow within food bins stacked in a pallet. PVC spheres were used to represent the horticultural products and a hot-wire anemometer measured the air velocity. The results showed preferential airflow pathways through the bins, along with back-mixing zones at the inlet corners. This uneven distribution of the flow was then directly related to the significant differences (up to 40 %) in the heat transfer coefficients measured, resulting in non-uniform cooling of the produce.

Alvarez et al. (2003) used LDA to determine the semiempirical constants needed to numerically model the turbulent kinetic energy and the heat transfer process that develop within a porous structure of stacked spheres in vented boxes. By seeding water droplets ($2x10^{-6}$ m mean diameter) and incense smoke in the flow field the velocities upstream, downstream and in between stacked PVC spheres representing the produce were measured. The numerical model developed then identified maximum air velocities within the centre of the vented box and decreasing velocities towards the corners of the box, which could explain the cooling heterogeneity observed within the box.

Delele et al. (2008) used hot-wire anemometry to validate a CFD model for the forced-air cooling of a box containing 32 spheres representing horticultural produce. After validation the CFD model was used to simulate various scenarios (box vent hole ratio, product size, etc...). The results showed a decay in air velocity through the box, hence cooling potential, as the distance from the box inlet increased.

Delele et al. (2013b) measured the air velocity flowing through vented packages of citrus fruit and the corresponding airflow resistance across a stack during a typical forced air cooling application. The experimental data, obtained by using a hot-wire thermal anemometer and a differential pressure transmitter, was then used to validate a 3D CFD model of the forced-air cooling process. The CFD model showed that the cooling of individual pieces of produce was dependent on their location within the package. Produce near the package vents, specifically behind the entrance vents, experienced relatively high air velocities and, consequently, experienced the fastest cooling. Airflow homogeneity was found to improve with decreasing air velocity as the air flowed from the entrance to the exit vents in the package.

Recent studies into the packaging of table grapes have shown that the airflow can be significantly affected by the presence of inner packaging, such as carry-bags and liner films. Ngcobo et al. (2012) used a pressure transducer in a wind tunnel, simulating forced-air cooling, to show that liner films inside a ventilated package caused a significant increase in pressure drop (typically over 50 %) through ventilated packages of table grapes. Ngcobo et al. (2013) used a hot wire anemometer to measure the air velocity entering ventilated packages of table grapes stacked on a pallet during an experimental forced-air cooling set-up.

The pressure drop through the packages was also measured using a pressure transducer device. Results showed that the inner packaging significantly restricted the airflow through the box.

Using airflow resistance measurements from previous work Delele et al. (2013a) generated a CFD model of room cooling of table grape packages. The study showed that the half cooling times were increased by 61 % when a carry-bag was included in the package. Adding a liner film to the package, in addition to the carry-bag, further increased the half cooling time by 169 %.

3.2 Improvements to forced-air cooling operations

Dehghannya et al. (2008; 2011; 2012) investigated the size and location of vented areas on the cooling heterogeneity. A setup, involving a forced air tunnel to draw air through a bed of solid polymer balls, was designed to simulate postharvest cooling of spherical produce inside a ventilated package. A pitot tube recorded the air speed downstream of ventilated packages with a variety of vent areas open to incoming airflow, ranging from 2.4 % to 12.1%. The same airflow was pulled through each ventilated package allowing the effect of the vent area on the cooling profile to be evaluated. Results indicated that while cooling uniformity increases with the increase in vent area the rate of cooling is more dependent on the distribution of the vent areas and may actually be lower if the vents are not distributed properly. The cooling rate can be improved, for the same overall vent area, if the vents are evenly distributed along the package wall. For example, three vents, with one vent located near both edges of the package wall and one at the centre will facilitate a faster cooling rate then if the same three vents are located beside each other in the centre of the package wall (Dehghannya et al., 2012). The evenly distributed configuration promotes a more homogeneous distribution of the airflow throughout the package, hence faster cooling.

Using a previous developed and experimentally validated CFD model Delele et al. (2013c) analysed the effect of the area, shape, number and position of package vents on the forced-air cooling of packed produce. For a given airflow rate, the cooling rate and airflow uniformity were found to improve with an increase in the vent area up to 7 %. For a given pressure drop across the system, cooling rates were found to improve as the vent area increases, with the highest decrease in cooling time observed for an increase in vent area from 1 % to 3 % and the cooling rate becoming less sensitive to increases in vent area after 7 %. The airflow and cooling uniformity, but not cooling rate, could be improved by increasing the number of vents, even if the total vent area was kept constant. Changing the location of vents from the centre of the package to the top and bottom sections would change the location of the coldest sections but not cooling rate or uniformity while the cooling rate and uniformity was unaffected by the vent shape.

In order to improve upon the forced-air cooling of strawberry clamshells Ferrua and Singh (2008) developed an optically transparent model, representative of retail clamshells of strawberries to investigate the airflow behaviour. This model involved not only the use of a transparent solid material to reproduce the packaging structure (fused silica) but also a perfect refractive index matching between it and the working fluid (a mineral oil mixture). This set-up allowed the airflow behaviour within the packaging system to be measured by PIV and was then used to validate a numerical model for the forced-air cooling process of fresh strawberries in commercial packages (Ferrua and Singh, 2009a; 2009b). The authors were then able to make recommendations for a future package design, such as periodically reversing the direction is pulled through the pallet, based on guidelines formulated from the developed CFD model. In particular they found that increasing the vent area of the clamshells, hence forcing more air through the clamshells will not necessarily lead to improvements in the cooling rate of the process. Forcing more air through the clamshells causes a faster increase in the air temperature along the system which has a significant and detrimental effect on the cooling rate of the clamshells located at the end of the system (Ferrua and Singh, 2009c). It was found that the cooling rate and uniformity of the process could be improved by decreasing the temperature of the air been delivered at the warmest points within the system. This was achieved by bypassing half the airflow entering the pallet structure into the second part of the pallet, ensuring a supply of refrigerated air to the warmest clamshells located in the back half of the pallet (Ferrua and Singh, 2011). By doing this a decrease of 6 % in the time taken for the warmest part of the pallet to reach seven-eights cooling was observed.

4. Design and efficiency of refrigeration

4.1.1 Room cooling

Refrigerated rooms for the storage of food produce constantly circulate refrigerated air to maintain the produce at a low temperature. During storage, pallets of horticulture produce are placed within a room where an evaporator-fan circulates and cools the air within the unit (Figure 4).

An uneven airflow distribution in refrigerated rooms (Figure 4) can result in centrally located bins receiving very little airflow (Amos, 2005) and low air speeds towards the rear of the room (Delele et al., 2009a), effects that could be associated with the presence of warm spots and temperature heterogeneity within the produce. Within the last decade a number of studies have been done to better understand the relationship that exists between the distribution of the airflow within the system and the rate and uniformity of the refrigeration process.

Amos (2005) used the tracer gas technique to identify the airflow patterns within a cool store filled with horticulture produce stacked in bins. Carbon monoxide sensors were placed in a cool store containing 622 bins. The sensors were placed in front of the evaporator, at the rear of the cool store and within 5 sections spread uniformly between the bins where determined. Carbon monoxide was then injected into a variety of positions within the cool store and the mean velocity was calculated from the time of arrival from the injection point to each sensor. The results showed an uneven distribution of air flow within the cool store with the top layers and side columns of bins experiencing the highest air speeds while bins located centrally experienced much lower airflows. These areas of low air velocity coincided with warm spots in the cool room.

Using hot-film omni-directional anemometers Delele et al. (2009a) investigated the velocity profile around a stack of 72 boxes uniformly distributed within two rows inside a cool store.

Results were used to validate a developed a multiscale CFD model of chicory root cool store to investigate how humidification intervals can reduce chicory root weight loss during cooling. The validated model clearly illustrated how the low velocity cooling towards the rear of room was unable to completely remove the heat of respiration from the produce.

4.1.1 Improvements to room cooling

Hellickson et al. (2003) used flow visualisation to study the air circulation during the postharvest cooling of apples and pears in a controlled atmosphere refrigerated storage room. Helium-filled soap bubbles where dispersed inside a commercial sized fruit storage room and the bubble motion recorded by video. The authors concluded that air-circulation and fruit cooling during this operation could be improved by ensuring a minimum space of 0.6 m between the rear walls and the bin stacks and a space of 0.2 m between the sidewalls and bin rows.

Using the developed multiscale CFD model of the chicory root cool store Delele et al. (2009b) tested potentially scenarios to improve the system. Numerical results suggested that elongating the air deflector to direct refrigerated air to the rear of the room and reducing the stack height to increase the free air space at the top of the room, would lead to an improvement in the cooling time and overall process efficiency.

4.2.1 Refrigerated transport trailers

For transport vehicles of horticulture produce, such as highway trailers and trucks, a top-air delivery system is employed to continuously circulate refrigerated air (Figure 5). Air is blown from the refrigeration unit at the front, over the top of the horticulture produce, down between the pallets and returns to the refrigeration unit at the front of the vehicle.

In refrigerated transport trailers the product temperature and homogeneity are directly controlled by the airflow patterns (Moureh et al., 2009c). Refrigerated air must be delivered to all parts of the container to compensate for heat fluxes through container walls and/or the heat of respiration of the product. To understand airflow patterns in refrigerated transport trailers Moureh et al. (2004) constructed a reduced-scale model (1:3.3) of a refrigerated truck, containing slotted boxes filled with spheres, to validate a CFD model of the airflow within it. Atomised oil particles of 4 μm mean diameter were seeded in the airflow and LDA was used to measure the air velocity at 1,110 points. Moureh et al. (2009a) used this technique when studying the airflow in slot-ventilated enclosures partially filled with vented boxes, such as refrigerated transport trucks loaded with horticultural produce. The experiments as well as numerical results showed that air circulation was found to be dependent on the porosity of the boxes. For ventilated packages the refrigerated air supply jet had an increased penetration depth along the truck length compared to non-permeable boxes. Non-permeable boxes promoted short-circuiting of the airflow in the front part of the truck. This allowed produce in the front of the truck to receive a sufficient supply of refrigerated air to maintain the produce at low temperatures and remove the heat of respiration. However, the airflow rate was inadequate to produce located at the back of the truck promoting temperature heterogeneity within the truck.

4.2.2 Improvements to refrigerated transport trailers

Air-ducts located at the ceiling of refrigerated trucks can improve the overall homogeneity of the airflow, and consequently temperature, in the truck (Moureh et al., 2009c). When air-ducts are included the airflow is blown into the truck at three positions (at the front, 1/3 of the truck length from the front and 2/3 of the truck length from the front). The authors combined experimental and numerical work to show that the use of air-ducts avoids the occurrence of stagnant zones and low velocities in the rear (region furthest from the evaporator fan) of the truck, while reducing the air velocities at the front. Air-ducts were shown to prevent over-chilling of produce, due to high air velocities, in the front of the trailer and overheating of the produce, due to low air velocities, at the rear of the trailer.

4.3.1 Refrigerated display cabinets/domestic refrigerators

In open refrigerated display cabinets (Figure 6) and domestic refrigerators cooled air, at a low airflow rates, is circulated to the refrigerator shelves. In open refrigerated display cabinets (typically found in retail stores) warm air from outside is constantly infiltrating the cabinet, although an air curtain can reduce the amount, while in domestic refrigerators this occurs each time the door is opened.

By tracing a continuous and uniform injection of CO_2 gas Amin et al. (2009) investigated the amount of warm air infiltration into an open refrigerated display cabinet. The concentration of the tracer gas was measured at the discharge air grille, return air grille and the ambient outside environment. By finding the percentage of tracer gas that escapes to the ambient a relationship between tracer gas concentration and the amount of air infiltration can be established. Depending on the amount, this warm air infiltration can cause significant temperature heterogeneity within the cabinet resulting in temperature differences between the food products.

PIV has been used to characterise the air flow behaviour that develops from natural convection within a transparent model of a domestic refrigerator and its influence on water evaporation (Laguerre et al., 2008; 2009). By analysing the dynamics of smoke particles (generated using a low-temperature water-glycol mixture to seed the airflow) the authors showed the occurrence of natural convection within the refrigerator, with warm air flowing to the top of the refrigerator and cool air flowing to the bottom. In addition, the experimental results were used to validate a CFD model that simulated the simultaneous heat and moisture transfer in the refrigerator. By using the validated model Laguerre et al. (2010) showed the dehydration of the food product near the top the refrigerator due to the higher air temperature. Likewise, as the air flowed down towards the bottom of the refrigerator its temperature decreased resulting in condensation on the food products in this region. Further work by Laguerre et al. (2012) uses PIV to measure the air velocity profiles in a vertical open refrigerated display cabinet. The results showed the highest air velocity near the air supply and return ducks. As a consequence, due to the higher heat transfer coefficients, the temperature of food products located in these areas was particularly affected by the temperature of the air flowing past compared to the food located at the top of the display cabinets.

4.3.2 Improvements to open refrigerated display cabinets

The infiltration rate of warm air into display cabinets can be minimised by reducing the cabinet height and adjusting the angle of the jet nozzle supplying refrigerated air (Amin et al. (2011; 2012). By tracing a continuous and uniform injection of CO_2 Amin et al., (2011, 2012) used the previously developed tracer gas approach to relate primary curtain design parameters, such as the height of the opening and flow rate ratio, and secondary variables, including space between shelves filled with food products, to the infiltration rate of open refrigerated cavities. In particular the authors found that the infiltration rate was dependent on interacting variables. For example an extreme infiltration point could be reached by varying the height of the cabinet and the throw angle, the angle of the jet nozzle supplying refrigerated air relative to a vertical line through the cabinet.

5. Design and efficiency of drying operations

5.1 Understanding of convective drying systems

Drying operations use warm, dry air to lower the moisture content of horticulture produce. Although there are many set-up methods for drying food, in a typical forced convection dryer heated air is vertically blown across a bed of produce supported by a mesh (Figure 7). During the drying of a bed of horticultural produce the distribution of the warm air before it encounters the product (Janjai et al., 2006) and the bed depth and porosity (Lawrence and Maier, 2011) impact upon the overall drying efficiency. For impingement jet drying technology the number of jets, airflow exiting the jets and food product location relative to the nozzle(s) impact upon the drying rate and uniformity (Macroft & Karwe, 1999; Macroft et al., 1999).

To understand airflow distribution in a conventional longan dryer Janjai et al. (2006) manually moved a hot-wire anemometer to different points on a predetermined grid. The results showed that the airflow distribution was not symmetric with respect to the position of the warm air inlet. Regions directly to the left and right of the air inlet were found to receive very little airflow and consequently experienced low drying rates, leading to non-uniform drying of the produce.

Lawrence and Maier (2011) used a vane anemometer to measure the air velocity at the grain surface at four locations near the centre of grain bins as well as near the periphery at four cardinal (north, south, east and west) directions. The results showed a non-uniform distribution of the air within the system and were used to validate a CFD model of the process. Results from the CFD model showed that the depth and porosity of the bed can have a major impact on the airflow distribution within the bed and the overall efficiency of the drying process. Lower porosity and greater bed depths result in a higher resistance to airflow and consequently an uneven airflow distribution, which causes non-uniform drying.

LDA was used to analyse the axial and radial air velocity components in a commercial jet impingement oven, used for conventional drying or toasting, from a single jet (Marcroft & Karwe, 1999), and multiple jets (Marcroft et al., 1999). In both cases sublimed CO_2 (dry ice fog) was used as the seeding particles. It was found that when using multiple jets the food product, on a conveyer belt would experience uneven heating rates as it passed under multiple jets. When the food product was directly under jet it experiences a high air velocity, leading to heat transfer rates 2 to 3 times higher than when the product is not under the any jet, and hence experience smaller air velocities. Hence, the areas of the food product receiving the higher heat transfer rates dry quicker than the other areas of the product.

5.2 Improvements to forced convection drying systems

Nagle et al. (2010) used the portable hand held vane anemometer to record the velocity distribution at a drying facility as a way to investigate the effect of different modifications, such as a mesh to redirect the airflow, on the quality and energy performance of a hot air convection fixed-bed longan dryer. The air speed at the top of the produce bulk (25 cm depth) was determined, at 25 points in a 5x5 grid, at the beginning, middle and end of three drying operations where the inclusion of an inverted mesh evenly distributed the incoming airflow before it reached the produce. By improving the airflow distribution within the bed of products to be dried the mesh improved the uniformity of drying and overall dryer performance.

Janjai et al. (2006) increased the space under the perforated floor of a convective dryer and installed air guides after the air inlet to redirect the airflow. This improved the airflow distribution and hence drying uniformity of the process.

Sarkar and Singh (2004) used flow visualisation when investigating the relative importance of nozzle exit velocity, nozzle design and impingement equipment design on food processing, such as drying, using air impingement technology, consisting of jets emitting high-velocity air. A custom-built air impingement system allowed various nozzles sizes and equipment designs to be tested. Helium filled bubbles were introduced into the plenum and a camera was used to track the flow pattern of the jets. Experimental results showed that major improvements could be made to the air impingement systems drying performance by optimising the height to diameter ratio, in the region of 6-8, of the air jets and using fully developed jets.

6. Conclusions

For forced-air cooling, refrigeration and drying an even delivery of the airflow to each area of the system is essential to optimizing the performance of the operations. In forced-air cooling preferential airflow pathways, which cause significant differences to the air speeds within ventilated packages, and an inadequate delivery of cool air to packages centrally located and at the rear of pallets result in cooling heterogeneity in the system. The cooling rate can be improved by increasing the vent area to certain percentage, specific to each package while airflow and cooling uniformity can be improved by increasing the number of vents. In room cooling and refrigerated transport trailers pallets located furthest from the evaporator fans receive a small volume of the total airflow, resulting in the presence of warm spots at these locations. In open refrigerated display cabinets localised high air speeds and warm air infiltration can result in a fluctuating air temperatures, and consequently fluctuating food product temperatures. Uneven airflow distribution causes non-uniform bed drying while the location of the food product to impingement jets can cause uneven drying rates along the width of the produce.

In order to improve these systems airflow measurements which can identify areas receiving maximum and minimum airflow rates must be identified. While on-site measurements will always remain important, non-intrusive quantitative techniques like LDA and PIV can validate numerical models which can then be used to predict the product temperature and storage life depending on the initial and environmental conditions.

Acknowledgements

This review is an output of the PhD research of Justin O'Sullivan as supported by a Zespri™ International PhD scholarship.

References

Adrian, R. (1991). Particle-imaging techniques for experimental fluid mechanics, *Annual Review of Fluid Mechanics*, (23), 261-304.

Alvarez, G. & Flick, D. (1999a). Analysis of heterogeneous cooling of agricultural products inside bins Part I: aerodynamic study. *Journal of Food Engineering*, 39(3), 227-237.

Alvarez, G. & Flick, D. (1999b). Analysis of heterogeneous cooling of agricultural products inside bins Part II: thermal study. *Journal of Food Engineering*, 39(3), 239-245.

Alvarez, G., Bournet, P.E. & Flick, D. (2003). Two-dimensional simulation of turbulent flow and transfer through stacked spheres. *International Journal of Heat and Mass Transfer*, 46(13), 2459-2469.

Amanlou, Y., & Zomorodian, A. (2011). Evaluation of air flow resistance across a green fig bed for selecting an appropriate pressure drop prediction equation. *Food and Bioproducts Processing*, 89(2), 157-162.

Amin, M., Dabiri, D. & Navaz, H.K. (2009). Tracer gas technique: A new approach for steady state infiltration rate measurement of open refrigerated display cases. *Journal of Food Engineering*, 92(2), 172-181.

Amin, M., Navaz, H.K., Kehtarnavaz, N. & Dabiri, D. (2010). A systematic approach for solving large-scale problems by neural network: open refrigerated display cases and droplet evaporation problems. *Food and Bioprocess Technology*, 3(2), 276-287.

Amin, M., Dabiri, D. & Navaz, H.K. (2011). Comprehensive study on the effects of fluid dynamics of air curtain and geometry, on infiltration rate of open refrigerated cavities. *Applied Thermal Engineering*, 31(14-15), 3055-3065.

Amin, M., Dabiri, D. & Navaz, H.K. (2012). Effect of secondary variables on the infiltration rate of open refrigerated vertical display cabients with sinle-band air curtain, *Applied Thermal Engineering*, 35, 120-126.

Amos, N.D. (2005). Characterisation of air flow in a commerical cool store using a carbon monoxide gas tracer tracer technique. *Acta Hort*, 687, 305-312.

Ashby, B.H. (1995). Protecting perishable foods during transport by truck. *Handbook no. 669.* USDA. Washington, D.C.

Biwole, P.H., Yen, W., Yanhui, Z. & Roux, J-J. (2009). A complete 3D particle tracking algorithm and its applications to the indoor airflow study. *Measurement Science and Technology*, 20(115403), 13

Brosnan, T., & Sun D-W. (2001). Precooling techniques and applications for horticultural products – a review. *International Journal of Refrigeration*, 24(2), 154-170.

Carpentieri, M., Robins, A.G. & Baldi, S. (2009). Three-dimensional mapping of air flow at an urban canyon intersection. *Boundry-Layer Meteorology*, 133(2), 277-296.

Cornaro, C., Fleischer, A.S. & Goldstein, R.J. (1999). Flow visualization of a round jet impinging on cylindrical surfaces. *Experimental Thermal and Fluid Science*, 20(2), 66-78.

Coulson, J. M., Richardson, J. F., Backhurst, J. R. & Harker, J. H. (1999). *Coulson & Richardson's Chemical Engineering, Volume 1: Fluid Flow, Heat Transfer & Mass Transfer* (6th ed., pp. 232-273). Oxford.

de Castro, L.R., Vigneault. C., Cortez, L.A.B. (2004). Container opening design for horticulture produce cooling efficiency, *Journal of Food Agriculture and the Environment*, 2(1), 135-140.

Dehghannya, J.M., Ngadi, M. & Vigneault, C. (2008). Simultaneous Aerodynamic and Thermal Analysis during Cooling of Stacked Spheres inside Ventilated Packages, *Chemical Engineering Technology*, 31(11), 1651-1659

Dehghannya, J.M., Ngadi, M. & Vigneault, C. (2011). Mathematical modeling of airflow and heat transfer during forced convection cooling of produce considering various package vent areas, *Food Control*, 22(8), 1393-1399.

Dehghannya, J.M., Ngadi, M. & Vigneault, C. (2012). Transport phenomena modelling during produce cooling for optimal package design: Thermal sensitivity analysis, *Biosystems Engineering*, 111(3), 315-324.

Defraeye, T., Lambrecht, R., Delele, M.A., Tsige, A.A, Opara, U.L., Cronjé, P., Verboven, P. & Nicolaï, B.M. (2013). Forced-convective cooling of citrus fruit: package design, *Journal of Food Engineering*, 121, 118-127.

Defraeye, T., Lambrecht, R., Delele, M.A., Tsige, A.A, Opara, U.L., Cronjé, P., Verboven, P. & Nicolaï, B.M. (2014). Forced-convective cooling of citrus fruit: cooling conditions and energy consumption in relation to package design, *Journal of Food Engineering*, 121, 118-127.

Delele, M.A., Jaeken, P., Debaer, C., Baetens, K., Endalew, A.M., Nicolai, B.M. & Verboven, P. (2007). CFD prototyping of an air-assisted orchard sprayer aimed at drift reduction, *Computers and Electronics in Agriculture*, 51(1), 16-27.

Delele, M.A., Tijskens, E., Atalay, Y., Ho, Q., Ramon, H., Nicolaï, B.M. & Verboven, P. (2008). Combined discrete element and CFD modelling of airflow through random stacking of horticultural products in vented boxes, *Journal of Food Engineering*, 89(1), 33-41

Delele, M.A., Schenk, A., Tijskens, E., Ramon, H., Nicolai, B.M. & Verboven, P. (2009a). Optimization of the humidification of cold stores by pressurized water atomizers based on a multiscale CFD model, *Journal of Food Engineering*, 91(2), 228-239.

Delele, M.A., Schenk, A., Ramon, H., Nicolai, B.M. & Verboven, P. (2009b). Evaluation of a chicory root cold store humidification system using computational fluid dynamics, *Journal of Food Engineering*, 94(1), 110-121.

Delele, M.A, Ngcobo, M.E.K., Opara, U.L., & Meyer, C.J. (2013a). Investigating the Effects of Table Grape Package Components and Stacking on Airflow, Heat and Mass Transfer Using 3-D CFD Modelling. Food and Bioprocess Technology. *Food Bioprocess Technology*, 6(9), 2571-2585.

Delele, M.A, Ngcobo, M.E.K., Getahun, S.T., Chen, L., Mellmann, J. & Opara, U.L. (2013b). Studying airflow and heat transfer characteristics of horticultural produce packaging system using 3-D

CFD model, part I: model development and validation. *Postharvest Biology and Technology*, 86, 536-545.

Delele, M.A, Ngcobo, M.E.K., Getahun, S.T., Chen, L., Mellmann, J. & Opara, U.L. (2013c). Studying airflow and heat transfer characteristics of a horticultural produce packaging system using 3-D CFD model, part II: effect of package design. *Postharvest Biology and Technology,* 86, 546-555.

Dincer, I. (1995). Air flow precooling of individual grapes. *Journal of Food Engineering,* 26(2), 243-249.

Durst, F., Melling, A. & Whitelaw, J.H. (1981). Principles and Practice of Laser-Doppler Anemometry. London.

Ferrua, M.J. & Singh, R.P. (2008). A nonintrusive flow measurement technique to validate the simulated laminar fluid flow in a packed container with vented walls, *International Journal of Heat and Fluid Flow,* 31(2), 242-255.

Ferrua, M.J. & Singh, R.P. (2009a). Modeling the forced-air cooling process of fresh strawberry packages, Part I: Numerical model, *International Journal of Heat and Fluid Flow,* 32(2), 335-348.

Ferrua, M.J. & Singh, R.P. (2009b). Modeling the forced-air cooling process of fresh strawberry packages, Part II: Experimental validation of the flow model, *International Journal of Heat and Fluid Flow,* 32(2), 349-358.

Ferrua, M.J. and Singh, R.P. (2009c). Design guidelines for the forced-air cooling process of strawberries, *International Journal of Heat and Fluid Flow*, 32(8), 1932-1943.

Ferrua, M.J. and Singh, R.P. (2011). Improved airflow method and packaging system for forced-air coolnig of strawberry packaging, *International Journal of Refrigeration,* 34(4), 1162-1173.

Fingerson, L.M. & Freymuth, P. (1996). *Fluid Mechanics Measurements* (2^{nd} ed., pp 115-173). Washington, USA.

Foster, A.M., Barrett, R., James, S.J. & Swain, M.J. (2002). Measurement and prediction of airflow movement through doorways in refrigerated rooms, *International Journal of Refrigeration*, 25(8), 1102-1109.

Ghisalberti, L. & Kondjoyan, A. (1999). Convective heat transfer coefficients between air flow and a short cylinder. Effect of air velocity and turbulence. Effect of body shape, dimensions and position in the flow, *Journal of Food Engineering*, 42(1), 33-44.

Gijsen, F.J.H., Palmen, D.E.M., van der Beek, M.H.E., van de Vosse, F.N., van Dongen, M.E.H. & Janssen, J.D. (1996). Analysis of the axial flow field in stenosed carotid artery bifurcation models-LDA experiments, *Journal of Biomechanics*, 29(11), 1483-1489.

Gill, R.S., Singh, S. & Singh, P.P. (2012). Design and development of desiccant seed dryer with airflow inversion and recirculation, *Journal of Food Science and Technology*

Hossain, M.A. & Bala, B.K. (2007). Drying of hot chilli using solar tunnel drier. *Solar Energy*. 81(1), 85-92.

Hellickson, M.L. & Baskins, R.A. (2003). Visual documentation of air flow patterns in a controlled atmosphere storage, *Acta Hort*, 600, 173-179.

Janjai, S., Intawee, P., Chaichoet, C., Mahayothee, B., Haewsungcharern, M. & Muller, J. (2006). Improvement of the air flow and temperature distribution in a conventional longan dryer. *International Symposium Towards Sustainable Livelihoods and Ecosystems in Mountainous Regions*, Chiang Mai, Thailand.

Jeffrey, D., Zhang, X., & Hurst, D.W. (2000). Aerodynamics of gurney flaps on a single-element high-lift wing, *Journal of Aircraft*, 37(2), 295-301.

Jing, X., Lu, J.Y.., Mioa, J.M., Hans, H., Rahman, H.A., Pan, S.S. & Norford, L. (2011). An aerodynamically efficient sphere anemometer with integrated hot-film sensors for 2-D environmental airflow monitoring. *16th International Conference on Solid-State Sensors, Actuators and Microsystems*, Beijing, China.

Jorgensen, F.E. (2002). How to measure turbulence with hot-wire anemometers – a practical guide. Dantec Dynamics.

Kadam, D.M., Nangare, D.D., Singh, R. & Kumar, S. (2008). Low-cost greenhouse technology for drying onion (allium cepa L.) slices. *Journal of Food Process Engineering*, 34, 67–82.

Kashaninejad, M., Maghsoudlou, Y., Khomeiri, M. & Tabil, L.G. (2010). Resistance to airflow through bulk pistachio nuts (Kalleghochi variety) as affected by moisture content, airflow rate, bed depth and fill method, *Powder Technology*, 203(2), 359-364.

Khatchatourian, O.A., Toniazzo, N.A. & Gortyshov, Y.F. (2009). Simulation of airflow in grain bulks under anisotropic conditions, *Biosystems Engineering*, 104(2), 205-215.

Khot, L. R., Ehsani, R., Albrigo, G,. Larbi, P.A., Landers, A., Campoy, J. & Wellington, C. (2012). Air-assisted sprayer adapted for precision horticulture: Spray patterns and deposition assessments in small-sized citrus canopies, *Biosystems Engineering*, 113, 76-85.

Klimentjew, D., Flick, N.E., Bosselmann, T. & Zhang, J. (2010). 3D hypergraph-oriented air flow analysis based on PTV. *International Conference on Information and Automation*, Harbin, China.

Kondjoyan, A. (2006). A review on surface heat and mass transfer coefficients during air chilling and storage of food products. *International Journal of Refrigeration*, 29(6), 863-875.

Kumar, R., Kumar, A. & Murthy, U.N. (2008). Heat transfer during forced air precooling of perishable food products, *Biosystems Engineering*, 99(2), 288-233.

Kumar, V., Wee, A.P., Birla, S., Subbiah, J. & Harshavardhan, T. (2012). A 3-D computational fluid dynamics model for forced air cooling of eggs placed in trays, *Journal of Food Engineering*, 108(3), 480-492.

Laguerre, O. & Flick, D. (2004). Heat transfer by natural convection in domestic refrigerators, *Journal of Food Engineering*, 62(1), 79-88.

Laguerre, O., Amara, S.B., Charrier-Mojtabi, M.-C., Lartigue, B. & Flick, D. (2008). Experimental study of air flow by natural convection in a closed cavity: Application in a domestic refrigerator, *Journal of Food Engineering*, 85(4), 547-560.

Laguerre, O., Remy, D. & Flick, D. (2009). Airflow, heat and moisture transfers by natural convection in a refrigerating cavity, *Journal of Food Engineering*, 91(2), 197-210.

Laguerre, O., Benamara, S. & Flick, D. (2010). Numerical simulation of simultaneous heat and moisture transfer in a domestic refrigerator, *International Journal of Refrigeration,* 33(7), 1425-1433.

Laguerre, O., Hoang, M.H., Osswald, V. & Flick, D. (2012). Experimental study of heat transfer and air flow in a refrigerated display cabinet, *Journal of Food Engineering*, 113, 310-320.

Lawrence, J. & Maier, D. E. (2011) Three-dimensional airflow distribution in a maize silo with peaked, levelled and cored grain mass configurations. *Biosystems Engineering*, 110(4), 321-329.

Lim, W.L., Chew, Y.T., Chew, T.C., & Low, H.T. (2001). Pulsatile flow studies of a porcine bioprosthetic aortic valve in vitro: PIV measurements and shear-induced blood damage, *Journal of Biomechanics,* 34(11), 1417-1427.

Lomas, C.G. (1986). *Fundamentals of hot wire anemometry*. New York

Madhiyanon, T., Piriyarungroj, N. & Soponronnarit, S. (2008). Cold flow behavior study in novel cyclonic fluidized bed combustor, *Energy Conversion and Management,* 49(5), 1202-1210.

Maghirand, R. G. & Manbeck, H. B. (1993). Modeling particle transport in slot-inlet ventilated airspaces. *Transactions of the ASABE,* 36(5), 1449-1459.

Marcroft, H.E. & Karwe, M.V. (1999). Flow field in a hot air jet impingement oven – part 1: a single impinging jet. *Journal of Food Processing and Preservation*, 23(3), 217-233.

Marcroft, H.E., Chandrasekaran, M. & Karwe, M.V. (1999). Flow field in a hot air jet impingement oven – part 2: multiple impingement jets. *Journal of Food Processing and Preservation*, 23(3), 235-248.

Mattingly, G. E. (1996). *Fluid Mechanics Measurements* (2nd ed., pp 301-366). Washington, USA.

McWilliams, J. (2003). Review of airflow measurement techniques, *AIVC Annotated Bibliography BIB 12,* www.aivc.org.

Mirade, P.S. & Daudin, J.D. (1998). A New Experimental Method for Measuring and Visualising Air Flow in Large Food Plants, *Journal of Food Engineering,* 36, 31-49.

Mohanraj, M. & Chandrasekar, P. (2008). Drying of copra in a forced convection solar dryer, *Journal of Food Engineering*, 99(4), 604-607.

Motevali, A., Younji, S., Amiri Chayjan, R., Aghilinategh, N. & Banakar, A. (2013). Drying kinetics of dill leaves in a convective dryer. *International Agrophysics*. 27, 39-47.

Moureh, J.M., Tapsoba, M. & Flick, D. (2009a). Airflow in a slot-ventilated enclosure partially filled with porous boxes: Part I – Measurements and simulations in the clear region. *Computers and Fluids,* 38(2), 194-205.

Moureh, J.M., Tapsoba, M. & Flick, D. (2009b). Airflow in a slot-ventilated enclosure partially filled with porous boxes: Part II – Measurements and simulations within porous boxes. *Computers and Fluids,* 38(2), 206-220.

Moureh, J. M., Tapsoba, M., Derens, E. & Flick, D. (2009c). Air velocity characteristics within vented pallets loaded in a refrigerated vehicle with and without air ducts. *International Journal of Refrigeration*, 38(2), 220-234.

Mueller, T. J. (1996). *Fluid Mechanics Measurements* (2^{nd} ed., pp 367-508). Washington, USA.

Nagle, M., Carlos, J.C.A, Mahayothee, B., Haewsungcharern, M, Janjai, S. & Müller, J. (2010). Improved quality and energy performance of a fixed-bed longan dryer by thermodynamic modifications, *Journal of Food Engineering*, 99(3), 392-399.

Ngcobo, M.E.K., Delele, M.A, Opara, U.L., Zietsman, C.J. & Meyer, C.J. (2012). Resistance to airflow and cooling patterns through multi-scale packaging of table grapes. *International Journal of Refrigeration*, 35(2), 445-452.

Ngcobo, M.E.K., Delele, M.A, Opara, U.L. & Meyer, C.J. (2013). Performance of multi-packaging for table grapes based on airflow, cooling rates and fruit quality. *Journal of Food Engineering*, 116(2), 613-621.

Nijhuis, H.H., Torringa, H.M., Muresan, S., Yuksel, D., Leguijt, C. & Kloek, W. (1998). Approaches to improving the quality of dried fruti and vegetables. *Food Science and Technology*, 9(1), 13-20.

O'Sullivan, J.L., Ferrua, M.J., Love, R.J., Verboven, P., Nicolaï, B.M. & East, A.R. (2013) Performance of the forced-air cooling process of fruit packed in polyethylene liners as a function of pallet orientation, *Proc. 2^{nd} IIR International Conference on Sustainability and the Cold Chain*, Paris, France.

Page, J.-F. L., Chevarin, C., Kondjoyan, A., Daudin, J.D. & Mirade, J.D. (2009). Development of an approximate empirical-CFD model estimating coupled heat and water transfers of stacked food products placed in airflow, *Journal of Food Engineering*, 92(2), 208-216.

Pathare, P.B., Opara, U.L., Vigneault, C., Delele, M. & Al-Said, F.A. (2012). Design of packaging vents for cooling fresh horticultural produce, *Food and Bioprocess Technology*, 5(6), 2031-2045.

Prasad A.K. (2000). Particle image velocimetry. *Current Science*, 79(1), 51-60

Raffel, M. & Kost, F. (1998). Investigation of aerodynamic effects of coolant ejection at the trailing edge of a turbine blade model by PIV and pressure measurements, *Experiments in Fluids*, 24(5-6), 447-461.

Ramírez-Gilly, M., Martínez-Padilla, L.P. & Manero, O. (2007). Particle image velocimetry applied to suspensions of millimetric-size particles using a vane-in-a-large-baffled-cup rheometer, *Journal of Food Engineering*, 78(4), 1117-1126.

Rathakrishnan, E. (2007). *Instrumentation, Measurements, and Experiments in Fluids* (1^{nd} ed., pp 9-520). CRC Press.

Randall, J.M. & Battams, V.A. (1979). Stability Criteria for Airflow Patterns in Livestock Buildings. *Journal of Agricultural Engineering Research*, 24, 361-374.

Ruegg, T., Stangier, R., Stoeckli, B., Tanner, C., Dorer, V. & Lommel, A. (1994). 3D airflow velocity vector sensor. *Proc. Of Roomvent '94*, Krakow, Poland.

Sarkar, A. & Singh, R.P. (2004). Air impingement technology for food processing: visualisation studies. *Food Science and Technology*, 37(8), 873-879.

Santonico, M., Bellincontro, A., De Santis, D. Di Natale, C. & Mencarelli, F. (2010). Electronic nose to study postharvest dehydration of wine grapes, *Food Chemistry*, 121(3), 789-796.

Sherman, M.H. (1990). Tracer-gas techniques for measuring ventilation in a single zone. *Building and Environment*, 25(4), 365-374.

Smale, N. J., Moureh, J. M. & Cortella, G. (2006). A review of numerical models of airflow in refrigerated food applications. *International Journal of Refrigeration*, 29(6), 911-930.

Suzuki, Y. & Kasagi, N. (2000). Turbulent Air-Flow Measurement with the Aid of 3-D Particle Tracking Velocimetry in a Curved Square Bend. *Flow, Turbulence and Combustion*, 63(1), 415-442.

Tanner, D. J., Cleland, A.C., Roberston, T.R. & Opara, L.U. (2000). Use of Carbon Dioxide as a Tracer Gas for Determining In-package Airflow Distribution. *Journal of Agricultural Engineering Research*, 77(4), 409-417.

Tapsoba, M., Moureh, J.M. & Flick, D. (2007). Airflow patterns in a slot-ventilated enclosure partially loaded with empty slotted boxes. *International Journal of Refrigeration*, 28(5), 963-977.

Tutar, M., Erdogdu, F. & Toka, B. (2009). Computational modeling of airflow patterns and heat transfer prediction through stacked layers' products in a vented box during cooling. *International Journal of Refrigeration* 32(2): 295-306.

Verboven, P., Hoang, M.L. & Nicolai, B.M. (2003). Modelling turbulent air flow in cool rooms for horticultural products. *Acta Hort,* 599, 435-441.

Verboven, P., Tijskens, E., Ramon, H. & Nicolai, B.M. (2005). Virtual filling and airflow simulation of boxes with horticultural products. *Acta Hort*, 687, 47-54.

Wang, A.-B., Tra´vnı´cˇek, Z. & Chia, K.-C. (2000). On the relationship of effective Reynolds number and Strouhal number for the laminar vortex shedding of a heated circular cylinder. *Physics of Fluids*, 12(6), 1401.

Wang, L. & Sun, D.-W. (2003). Recent developments in numerical modelling of heating and cooling processes in the food industry—a review, *Trends in Food Science and Technology,* 14(10): 408-423.

Webster, J.G. (2000). *Mechanical Variables Measurement – Solid, Fluid, and Thermal*. Boca Raton, Florida.

Węcel, D., Chmielniak, T. & Kotowicz, J. (2008). Experimental and numerical investigations of the averaging Pitot tube and analysis of installation effects on the flow coefficient, *Flow Measurement and Instrumentation*, 19(5), 301-306.

Wu, H., Lin, B. & Morgan, M.N. (2007). Measurement of the air boundary layer on the periphery of a rotating grinding wheel using LDA, *Journal of Physics: Conference Series*, 76(1), paper no. 012059.

Yan, W., Zhang, Y., Sun, Y. & Li, D. (2009). Experimental and CFD study of unsteady airborne pollutant transport within an aircraft cabin mock-up, *Building and Environment*, 44(1), 34-43.

Figures

Figure 1. Tunnel cooler, the most common forced-air cooling device. The fan creates a vacuum which draws refrigerated air through two palletized rows of horticulture produce.

Figure 2. Refrigerated storage room for horticulture produce. Evaporator fans circulate refrigerated air through the room.

Figure 3. Open refrigerated display cabinet.

Figure 4. Refrigerated truck with a top-air delivery system. Air is blown from the refrigeration unit at the front, over the top of the horticulture produce, down between the pallets and returns to the refrigeration unit at the front of the vehicle.

Figure 5. Forced convection dryer. Heated air is blown under a mesh which supports the horticultural produce.

Figure 6. Laser Doppler Anemometry measurement technique for measuring fluid velocity

Figure 7. Figure 7. Particle Image Velocimetry technique for measuring fluid velocity

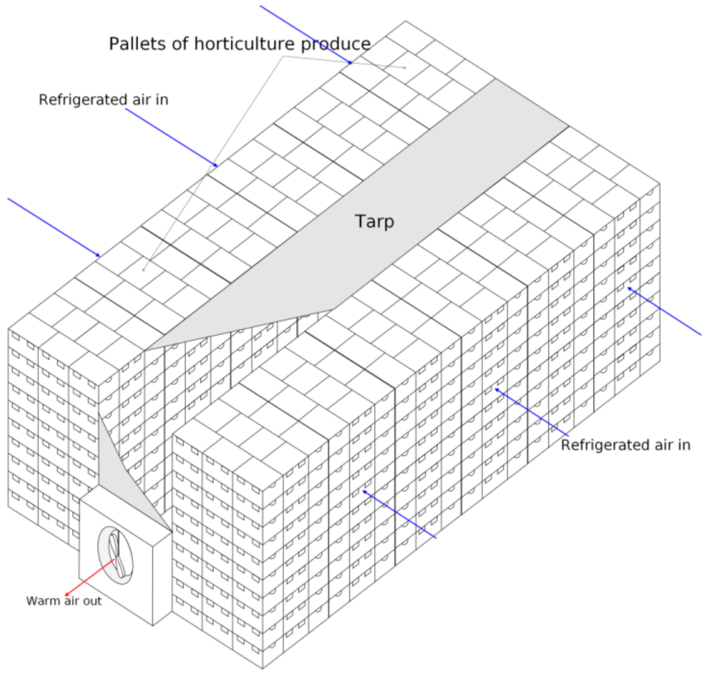

Figure 1. Tunnel cooler, the most common forced-air cooling device. The fan creates a vacuum which draws refrigerated air through two palletized rows of horticulture produce.

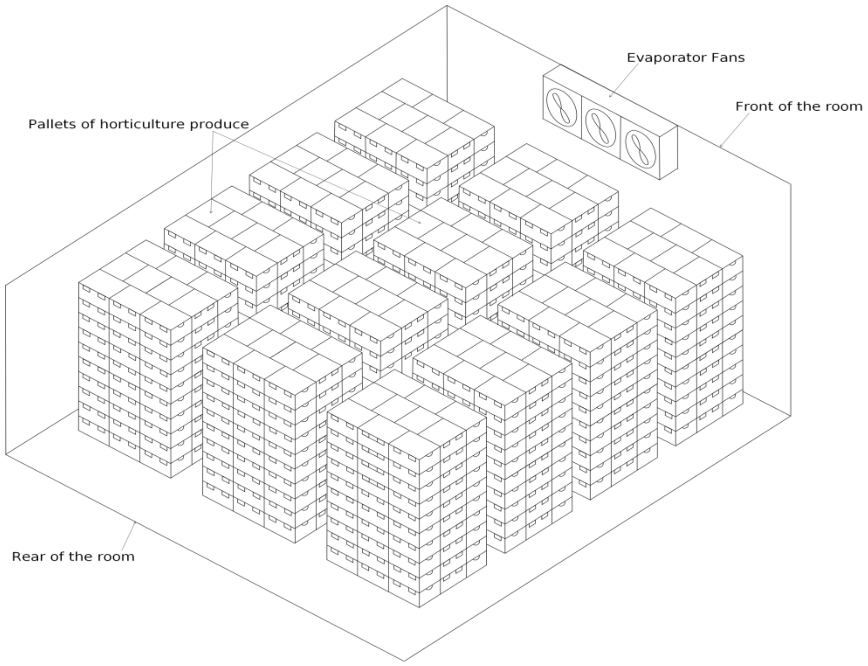

Figure 2. Refrigerated storage room for horticulture produce. Evaporator fans circulate refrigerated air through the room.

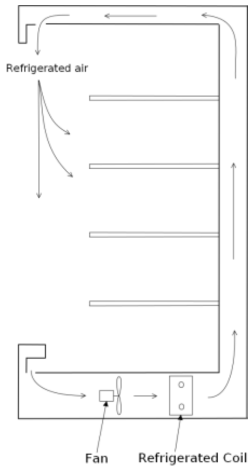

Figure 3. Open refrigerated display cabinet.

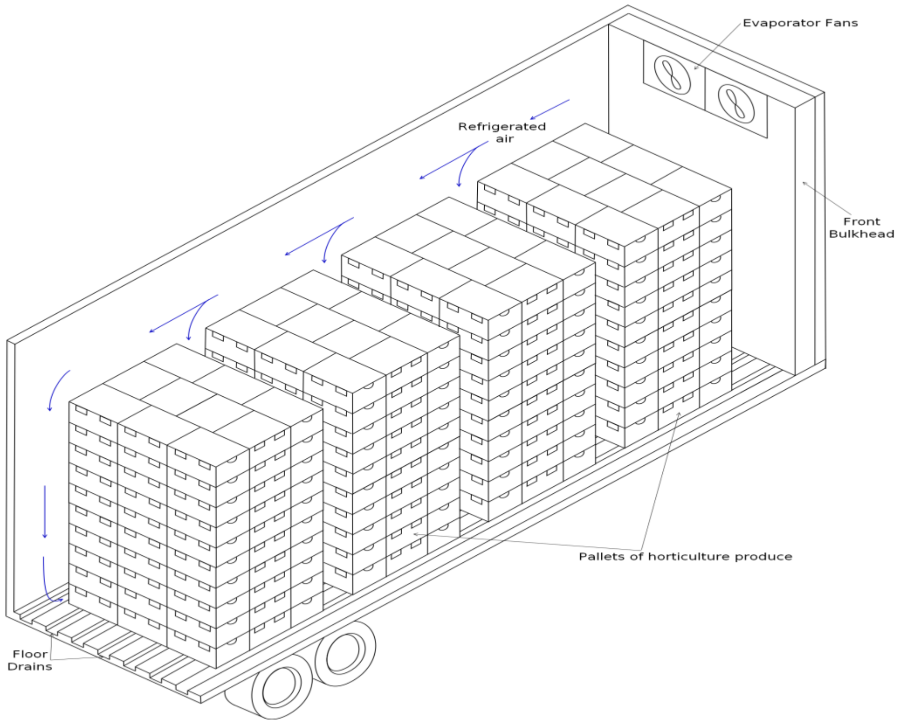

Figure 4. Refrigerated truck with a top-air delivery system. Air is blown from the refrigeration unit at the front, over the top of the horticulture produce, down between the pallets and returns to the refrigeration unit at the front of the vehicle.

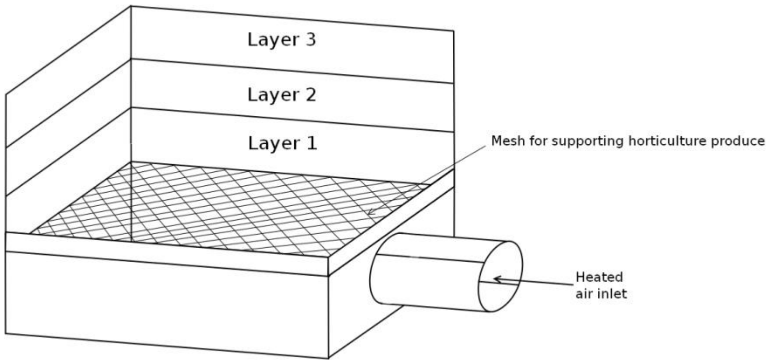

Figure 5. Forced convection dryer. Heated air is blown under a mesh which supports the horticultural produce.

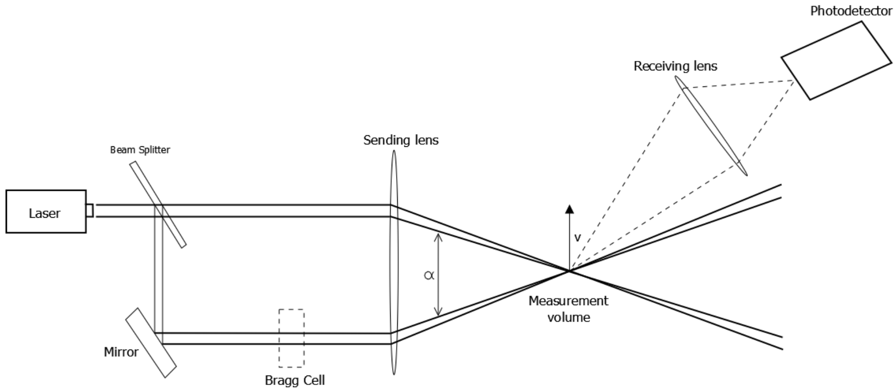

Figure 6. Laser Doppler Anemometry measurement technique for measuring fluid velocity

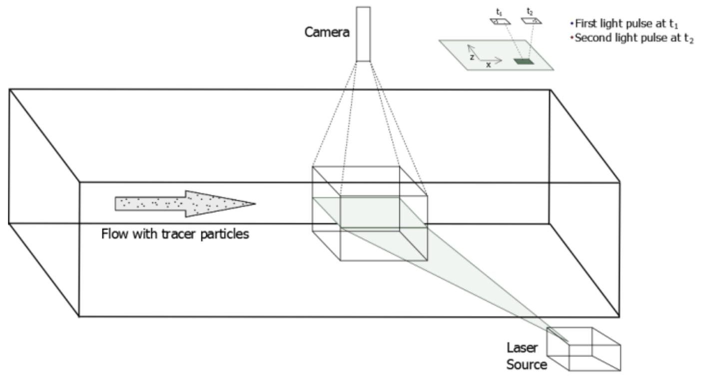

Figure 7. Particle Image Velocimetry technique for measuring fluid velocity